Quantitative Analysis of Coronal X-ray Spectra at High Resolution

Nancy S. Brickhouse

Smithsonian Astrophysical Observatory, 60 Garden St., Cambridge, MA, USA

ABSTRACT

We use Chandra observations to illustrate the X-ray spectral resolution and throughput required to probe the physical processes in stellar coronae. With today's capability, we are in a strong position to quantify the physical conditions (temperatures, abundances, and densities) for a number of stellar systems. The future holds the promise of dynamical studies to test the physical processes in the corona (heating, loop formation, winds).

Diagnostic studies include measurements of electron densities in cool star atmospheres. Published measurements of electron densities from Chandra and XMM-Newton in the brightest stellar coronae disagree by more than an order of magnitude. We show that reconciling these measurements requires detailed treatment of weak satellite spectra and other line blending. While these studies provide a sobering view of electron density measurements, they also provide a strong indication of what can be learned in the future when we combine high spectral resolution with high signal-to-noise.

Dynamic studies using Chandra HETG Doppler shifts are so far only reported for the most rapidly rotating cool stars. These new measurements are somewhat compromised by the presence of continuum and weak line blends, and are near the statistical limit. Nevertheless, they can provide a realistic test of the spectral synthesis such that the location(s) of coronal loops can be compared to the photospheric Doppler images. Examples of what can be learned from dynamic studies are presented.

Keywords: stars: coronae, techniques: spectroscopic, X-rays: stars

1. INTRODUCTION

In the X-ray emitting atmospheres of stars, a diversity of physical conditions allows us to explore the physical phenomena of flare production, coronal heating, magnetic reconnection, wind acceleration, and shocks. High resolution spectroscopy holds the key to determining not only the physical conditions (temperature, density, and elemental abundances) but also the dynamic effects of coronal phenomena.

This paper illustrates the spectral resolution and throughput needed with the next generation of X-ray satellites to address some of the important goals of stellar coronal physics. While high spectral resolution at Fe K (6 keV) achieved by microcalorimeters will facilitate studies of flares, other basic questions in coronal physics are best addressed at lower energy, where lines from the peak of the emission measure distribution are formed.

Further author information: E-mail: nbrickhouse@cfa.harvard.edu, Telephone: 617 495 7438

This paper was published in *X-Ray and Gamma-Ray Telescopes and Instruments for Astronomy*, Joachim E. Truemper and Harvey D. Tananbaum, Editors, Proceedings of SPIE Vol. 4851, p. 69, and is made available as an electronic reprint with permission of SPIE.

2. SPECTROSCOPY: THE SOLAR – STELLAR X-RAY CONNECTION

While the rich phenomenology of the *solar* corona can now be explored in exquisite detail with spectro-imaging techniques, many basic questions in coronal physics remain unanswered. Flaring loops are believed to be filled by evaporation of flare-heated chromospheric material; however, dynamic processes in flares as revealed by the widths and shifts of solar X-ray lines are not in good agreement with models.[1] Coronal loops observed in the EUV with TRACE and the EIT on SOHO appear more isothermal and overly dense compared with predictions from standard loop models, requiring non-uniform heating and probably deviations from hydrostatic equilibrium.[2] TRACE images of active region loops show no evidence for motions, yet simultaneous observations using the SUMER spectrometer on SOHO show flows $\sim$ 40 km s^{-1} in Ne VIII λ780.32 down the loop legs.[3] Doppler line shifts in Fe XIX λ1118.1 have recently been observed with SUMER above an active region, showing oscillations with a period 14–18 min and a decay time 12-19 min and indicating velocities as high as 77 km s^{-1}.[4] This line represents plasma significantly hotter than typical active region temperatures, though no indication of flaring is present. Modeling the effects of high-temperature flows in coronal loops may provide clues to coronal heating. While individual *stellar* coronal loops are not accessible through imaging techniques, some spectroscopic signatures of dynamic coronal processes have been discovered recently, suggesting rich possibilities for the future.

There are good reasons to look at stars beyond the Sun to explore coronal physics. One major reason is that stellar coronae offer a much larger parameter space in which to study physical processes. Giant flares on stars are orders of magnitude more energetic than solar flares,[5] producing total energies as high as 10^{37} ergs with temperatures up to 10^8 K. Stellar coronae observed with EUVE and more recently with Chandra and XMM-Newton (notably Capella[6] and β Ceti[7]) show remarkably narrow features at 6×10^6 – 10^7 K in their emission measure distributions, derived from emission line fluxes. These emission measure distributions are more "isothermal" than expected from classic loop models. X-ray light curves of flares have been able to constrain the sizes and locations of a few flares.,[8,9] indicating size scales smaller than the stellar radius. Line ratio diagnostics show evidence for densities as high as 10^{13} cm^{-3}, requiring small scales and pressures three orders of magnitude larger than solar active region pressures (though not unlike solar flare pressures).[10,11] These stellar characteristics are reminiscent of the overdense, isothermal solar loops and may require similar heating mechanisms. Finally the issue of flows can also be addressed on stellar systems. FUSE measurements of Fe XVIII λ974.9 in some late-type stars show broad profile components with non-thermal velocities as high as $\sim$ 100 km s^{-1}.[12]

Stellar coronae also offer a broad context in which to consider the relationship between dynamo action and magnetic activity. Optical Doppler images show high latitude active regions in rapidly rotating systems,[13,14] whereas the Sun shows only coronal holes near the poles. These "starspots" are surprisingly long-lived and stable, surviving more than 10 years on the RS CVn system HR 1099. It is believed that rapid rotation can deflect the magnetic flux poleward through Coriolis forces. Theoretical studies show that with increasing rotation rate, centrifugal forces on large magnetic loops lead to larger pressure and density and a less extended corona.[15] The EUVE spectrum and light curve of 44i Boo (a contact binary with orbital period of 6.4 hrs) provided the first evidence for quiescent polar emission.[16]

Determining the sizes and locations of coronal loops (both flaring and quiescent) is important for understanding the role of rotation, binarity, stellar type or other fundamental parameters in magnetic activity. We discuss in the next sections new X-ray spectroscopy results bearing on these questions.

3. LINE FLUX DIAGNOSTICS

Line flux measurements provide the fundamental diagnostics for determining emission measure distributions (i.e. the density of material emitted as a function of temperature), electron density, and relative elemental abundances. Emission measure distributions over a broad X-ray emitting temperature range have been constructed for many late-type star using the emission lines of highly ionized iron observed first with EUVE and now with the new X-ray spectrometers.

Elemental abundances are determined relative to the derived emission measure distribution. Observations using the Chandra and XMM-Newton gratings are providing the best information to date about stellar coronal abundance patterns. While EUVE observations could only access elements other than iron in the least active

stars observable,[17] the ASCA CCDs could not easily distinguish more than a few temperature components in the system, and thus could not differentiate abundance effects from temperature effects in the global spectral fit. In fact, one of the early surprises of high resolution stellar X-ray spectroscopy has been the extraordinarily high abundance of neon — up to 10 times solar — in active binaries,[18,19] a result which had only been suggested by ASCA. While we do not yet understand the physics underlying abundance fractionation as material is transported from the photosphere into the corona, it is important to determine the abundance anomaly patterns in order to make progress. Whatever the explanation, knowledge of elemental abundances is critical to the proper calculation of the radiative cooling. Radiative cooling is the one term out of three in the basic coronal energy balance that we can now determine with high accuracy, with heating and conduction remaining more elusive.

Electron densities are generally determined from the ratio of a weaker line to a strong resonance line, where the weak line cannot quickly decay radiatively, as in collisional excitation of low-lying metastable levels or fine-structure levels of the ground configuration. EUVE studies of iron line ratio diagnostics have provided some strong evidence for high electron densities; however, many efforts have been plagued by low signal-to-noise, potential blending of the lines at resolution $\lambda/\Delta\lambda \sim 300$, and inconsistencies among the densities derived from supposedly redundant diagnostics. Unfortunately, the early results from Chandra and XMM-Newton have not yet clarified the situation; even with Chandra and XMM the measurements are challenging.

Fig. 1 demonstrates the difficulty of making flux measurements for weak lines in the presence of continuum and weak line blending. The Chandra HETG and LETG spectra of the O VII resonance (r), intercombination (i), and forbidden (f) lines at 21.6, 21.8, and 22.1 Å, respectively, appear to be fit well by a model consisting of three Gaussian lines and a flat "eye-ball" continuum; however, the LETG fit gives a significantly lower value for the weak i line. We have modeled the continuum shape using the emission measure distribution derived from strong iron lines, and fit its normalization (essentially the hydrogen to iron abundance ratio) to line-free regions of the HETG spectrum, as determined from the line models. Both continuum and line models are calculated using APEC[20] V1.2.0 models which are available online*. The agreement between the normalized theoretical continuum and the "eye-ball" fit for HETG is excellent. If we use the same continuum model for the LETG spectral fit, we can recover the HETG f/i line ratio as well. The problem arises from weak lines being treated as continuum at LETG resolution. It is interesting to note that with the higher effective area of the LETG, the level of the weak line "pseudo-continuum" has sufficient counts to drive the fit. For this reason, an accurate model of the weak lines, not needed at the higher resolution of HETG, must be used at LETG resolution. Near the O VII triplet, the spectral band is relatively clean except for the dielectronic recombination (DR) and inner-shell excitation satellite lines of O VII itself, and we find good agreement between APEC models and the observations. While the agreement is reassuring in this case, there are no guarantees that models will be able to compensate for insufficient spectral resolution everywhere.

Densities derived from the various fits and data sets are shown in Fig. 2. While the line ratios only differ by 30%, the inferred electron densities vary from $\sim 10^9$ ($< 2 \times 10^9$) cm^{-3} to $2 \times 10^{10}(\pm 1 \times 10^{10})$ cm^{-3}. A similar discrepancy among measurements exists for the Mg XI f/i ratio,[11] useful at higher temperatures ($\sim 10^7$ K). Meanwhile, other diagnostics at 10^7 K appear to confirm the higher densities ($> 10^{12}$ cm^{-3}) found with EUVE. The fluxes measured for the EUV iron lines using the LETG, with 5 times the spectral resolution and roughly 4 times the effective area of EUVE, agree with the EUVE values.[11] As in the case of O VII, it is clear from a comparison of spectra at different resolution that careful continuum modeling and an evaluation of the weak line blending are needed to make accurate measurements of the Mg XI triplet lines.

Our current difficulties with measuring density diagnostic line ratios will undoubtedly be ameliorated somewhat by an assessment of spectral models such as APEC, in progress under the Emission Line Project.[27] Nevertheless, we should not assume that models can compensate for instrumental limitations. Fortunately, the data from Chandra and XMM can provide realistic tests of the models and help identify the trade-offs between bandpass, spectral resolution and effective area. For coronal physics the minimum requirement should ensure that density measurements on short-time scales during flares can be made directly from the lines of interest.

Beyond the minimum requirement is the more exciting possibility of obtaining line ratio diagnostics for transient processes. Such diagnostics are possible using satellite lines. Doschek's review[28] of X-ray spectroscopy

*http://cxc.harvard.edu/atomdb

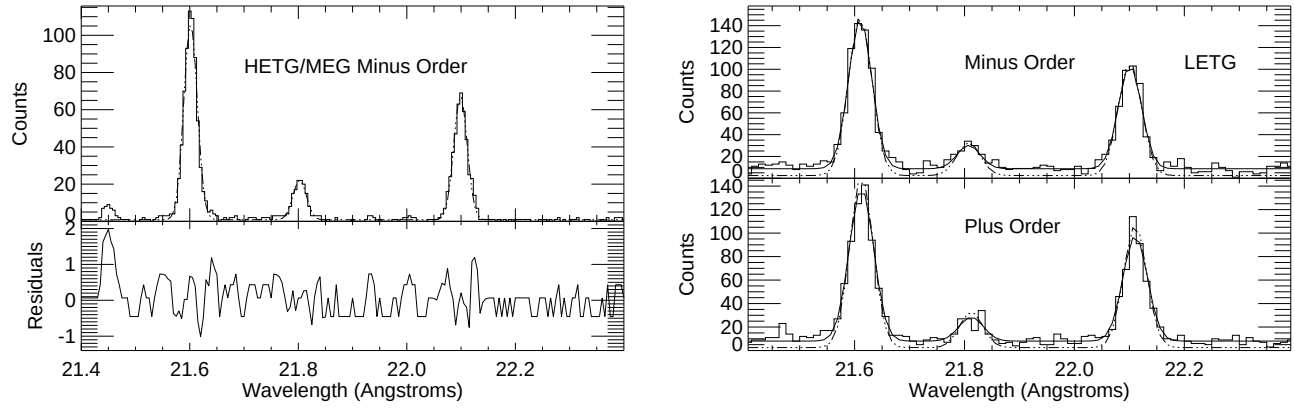

Figure 1. *Left:* Chandra HETG/ACIS-S MEG summed spectrum (minus first order) of Capella in the region of the O VII triplet lines, with a best fit model consisting of 3 Gaussian lines plus a flat continuum. The continuum level judged by eye agrees well with a continuum model fit to line-free regions throughout the spectrum. At this wavelength, $\lambda/\Delta\lambda = 950$ and $A_{eff} \sim 4$ cm^2. The exposure time of the summed spectrum is 154.7 ks. *Right:* Chandra LETG/HRC-S spectrum showing two fits, one with the continuum as a free parameter and the other with the continuum as determined for HETG. Note that the difference between these continuum models is accounted for by weaker unresolved lines in the spectrum, calculated in APEC and barely discernible in the MEG spectrum. $\lambda/\Delta\lambda = 440$ and $A_{eff} \sim 17$ cm^2. The exposure time is 85 ks.

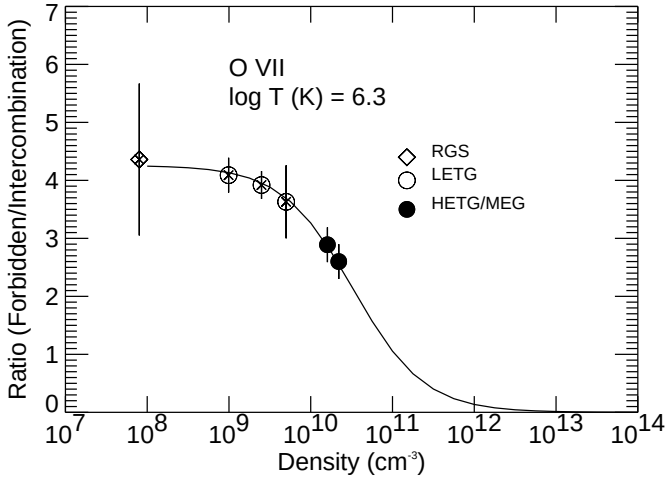

Figure 2. Published measurements of the O VII forbidden (f) to intercombination (i) line ratio observed in Capella. Measurements are ⋄ RGS[21] (52 ks); ∘ LETG[22–24] (92, 218, and 85 ks, in decreasing order); and • HETG[25,26] (89 and 68 ks). The solid curve is the corresponding APEC model.[20] The LETG fit with a proper continuum model (the lower curve in Fig. 1) comes into agreement with the HETG line ratio measurement.

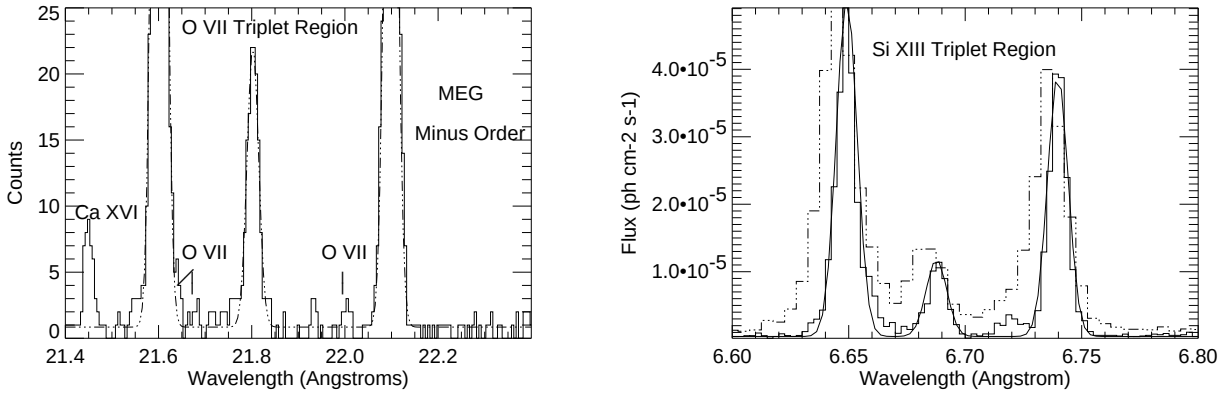

Figure 3. Chandra HETG summed spectra (histograms) of Capella with best fit models (smooth curves) consisting of 3 Gaussian lines plus a flat continuum for each spectral region shown. *Left:* MEG minus order (blown up from Fig. 1) showing detection of dielectronic recombination (DR) satellite lines of O VII relative to strong r, i, and f at 21.6, 21.8, and 22.1 Å, respectively, as predicted by theory.[29] *Right:* Solid histogram is the HEG (plus and minus orders co-added) spectrum of Si XIII. Satellite lines are again apparent (note the excess flux on the red wing of the resonance (r) line and the line blend apparent at 6.72 Å). $\lambda/\Delta\lambda = 610$ and the combined $A_{eff} \sim 60$ cm^2. The dash-dotted histogram is the MEG spectrum. With $\lambda/\Delta\lambda = 280$ the DR lines are not resolved by MEG. The MEG A_{eff} at this wavelength is 120 cm^2.

for solar flares contains a useful discussion on the diagnostic capabilities of satellite lines. The ratio of particular DR satellite lines to the He-like r line provides a sensitive temperature diagnostic during flare decay, which has been used to support the idea that some solar flares require continuous heating beyond the impulsive phase. The satellite line from inner shell excitation of Li-like ions (known as "q") can appear strong if the plasma is ionizing. By comparing a temperature-sensitive line ratio (e.g. q/r) to the temperature determined by the ratio of ionization states (essentially the contribution temperature, i.e. the temperature of the peak of the line emissivities integrated through the emission measure distribution) one can determine if the plasma is ionizing or recombining and thus begin to get a handle on the heating and cooling processes. Finally, solar spectra have been used to test the possibility of detecting non-Maxwellian velocity distributions using satellite lines, since the DR lines are formed only over a narrow (lower) energy range, whereas the collisionally excited lines are formed over the entire distribution and may be sensitive to "bumps on the tail" of the distribution.

Fig. 3 shows that the DR satellite lines of O VII are detected with MEG ($\lambda/\Delta\lambda \sim 950$). While the i and and f lines are useful as diagnostics of density, the DR satellites provide a sensitive probe of the temperature of the plasma. At 10^6 K in ionization equilibrium, the ratio of the strong DR line (on the red wing of the r line — see Fig.3) to the r line increases by a factor of 3 compared with the ratio at 2×10^6 K. This ratio is far more sensitive than the so-called G ratio ((i+f)/r) which only increases by 50 % over the same temperature range; however, it requires large effective area as well as good spectral resolution. For Si XIII, also shown in Fig. 3, the potential of the DR satellite lines for temperature diagnostics is even greater. The satellite line intensities become stronger relative to the r line for higher Z elements; furthermore, the close blend of Mg XII Ly$_\gamma$ with the Si XIII f line compromises the use of the f line.

4. LINE PROFILE DIAGNOSTICS

Line profile measurements provide information about the velocities of the ions. Thermal widths for coronal lines are generally below the resolution of the Chandra gratings; however, larger velocities can be observed. In principle, the blueshift from coronal evaporation during flare onset is observable, though no reports of a blueshifted X-ray line associated with flaring are known to this author. Doppler broadening from non-thermal processes (e.g. turbulence, rotation) is also observable for relatively large motions. With very high effective

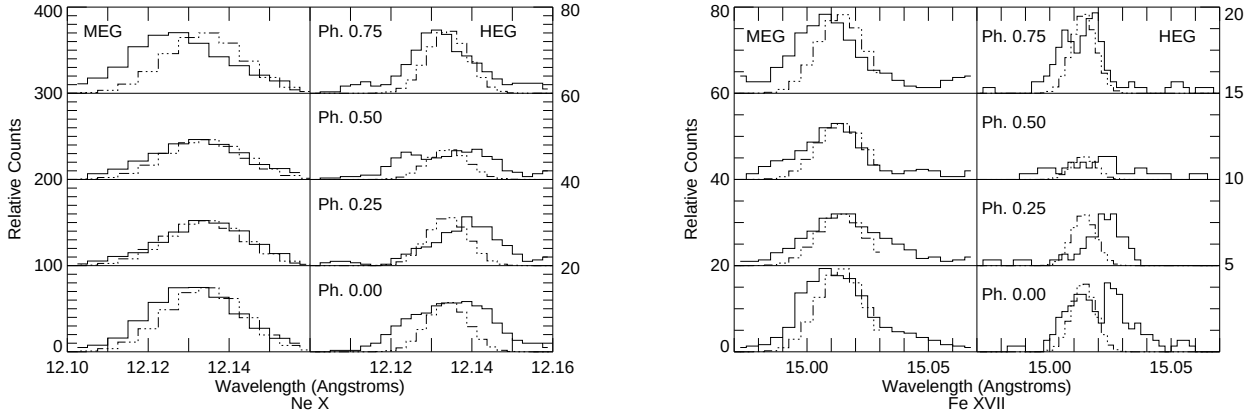

Figure 4. Ne X (*left*) and Fe XVII (*right*) line profiles of 44i Boo from Chandra MEG and HEG.[31] The zero points of the spectra are shifted up for each phase, but the scales are the same. The exposure time is not the same for each phase bin, so integrated counts will differ. For each profile, the instrumental line profile (dash-dotted histogram) is shown for comparison, with the peak set to the data peak and the centroid set at the laboratory wavelength. MEG line centroid shifts are measured, showing consistency with the motion of the primary star. The HEG profiles suggest additional velocity information, but the signal-to-noise is too low for quantitative analysis.

area, changes in the line profiles due to Doppler motions can be used to locate the emission. X-ray Doppler imaging holds great promise for studying dynamo action in stellar atmospheres. Schrijver[30] has argued recently that the smoothness of the solar magnetic fields implies that magnetic reconnection is a fast process, leaving the corona in a nearly potential-field configuration. A potential-field map determined from optical Doppler measurements can be extrapolated to predict the coronal emission, allowing comparison with X-ray Doppler maps. Understanding specifically the non-solar phenomenon of polar starspots may be key to understanding the relationship between photospheric magnetic fields and coronal loops in general.

Bulk motions have recently been observed in X-ray spectra, revealing velocities as low as ~ 150 km s^{-1}, as shown in Fig. 4, for the rapidly rotating contact binary 44i Boo.[31] Although this is an eclipsing system, the X-ray light curve shows no signature of either eclipse; however, there is a narrow dip in the light curve which repeats over 3 epochs and must be associated with rotational modulation. The phase-binned line profiles show centroid shifts associated with the motion of the primary star (Fig. 5). Using line profiles and light curves together, the analysis requires the emission to originate from a small-scale region near the pole of the primary star. These results confirm the previous EUVE period-search analysis.[16] Higher effective area with HEG resolution would facilitate tracking of multiple active regions on stars to perform true X-ray Doppler imaging. These studies in combination with ground-based photospheric and chromospheric measurements of starspots and magnetic fields will provide powerful tests of loop formation models.

5. CONCLUSIONS

The next generation of X-ray satellites will provide far greater effective area for X-ray spectroscopy across a broad spectral range, enabling stellar coronal studies to address the dynamics of coronal active regions and flares. The spectroscopy of stellar coronae is relatively mature (though the physical interpretation may not be) compared with our understanding of the spectra of active galaxies, X-ray binaries, supernova remnants, and other types of X-ray emitting sources. Thus the challenges of interpreting existing spectral data in the presence of imperfect models, demonstrated here, need to be taken seriously. Simulations of observing scenarios using spectral models are insufficient to judge whether the scientific goals can be met. We already have stellar coronal data in hand from Chandra and XMM which can be used as realistic benchmarks. These existing observations at the highest spectral resolution can serve as tests to ensure that the new instruments can meet the requirements for the future.

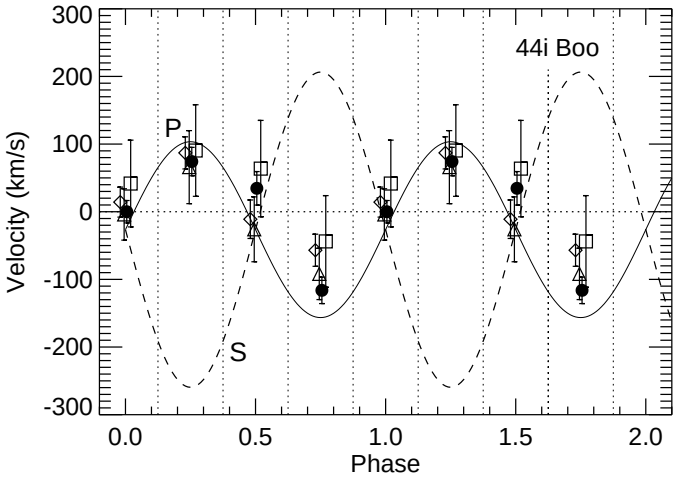

Figure 5. Velocities as a function of orbital phase, as measured from MEG profiles.[31] Velocities are derived from the median centroid shifts for the phase bins indicated by vertical dashed lines. The four symbols represent O VIII ($\diamond$), Ne X ($\bullet$), Fe XVII (Δ), and Mg XII ($\square$). Error bars represent statistical errors only. The different symbols are shifted slightly from their phase centers for plotting. Radial velocity curves for the primary (solid) and secondary (dash-dotted) are overplotted. Only four phase bins are measured with the available statistics. Error bars on centroids measured from HEG profiles are larger still due to lower signal-to-noise, while MEG profiles do not show any additional profile features (see Fig. 4).

ACKNOWLEDGMENTS

This work was supported in part by NASA grant NAG5-9986 and CXC NASA grant NAS8-39073 from NASA to the Smithsonian Astrophysical Observatory. The author wishes to acknowledge the Emission Line Project team and co-leader Jeremy Drake and the APEC team, especially Randall Smith.

REFERENCES

1. G. A. Doschek, "X-ray and EUV observations of solar flares," in *Stellar Coronae in the Chandra and XMM-Newton Era*, F. Favata and J. J. Drake, eds., *ASP Conf.* **in press**, 2002.
2. M. J. Aschwanden, C. J. Schrijver, and D. Alexander, "Modeling of coronal euv loops observed with TRACE. I. Hydrostatic solutions with nonuniform heating," *Ap J* **550**, pp. 1036–1505, 2001.
3. A. R. Winebarger, H. Warren, A. van Ballegooijen, E. E. DeLuca, and L. Golub, "Steady flows detected in extreme-ultraviolet loops," *Ap J* **567**, pp. L89–L92, 2002.
4. T. Wang, S. K. Solanki, W. Curdt, D. E. Innes, and I. E. Dammasch, "Doppler shift oscillations of hot solar coronal plasma seen by SUMER: A signature of loop oscillations?," *Ap J* **574**, pp. L101–L104, 2002.
5. F. Favata, "Giant x-ray stellar flaring events," in *Stellar Coronae in the Chandra and XMM-Newton Era*, F. Favata and J. J. Drake, eds., *ASP Conf.* **in press**, 2002.
6. A. K. Dupree, N. S. Brickhouse, G. A. Doschek, J. C. Green, and J. C. Raymond, "The extreme ultraviolet spectrum of Alpha Aurigae (Capella)," *Ap J* **418**, pp. L41–L44, 1993.
7. T. R. Ayres, T. Simon, R. A. Stern, S. A. Drake, S. B. E. Wood, and A. Brown, "The coronae of moderate-mass giants in the Hertzsprung Gap and the Clump," *Ap J* **496**, pp. 428–448, 1998.
8. C. S. Choi and T. Dotani, "ASCA observation of a long-duration x-ray flare from the W UMa–type binary VW Cephei," *Ap J* **429**, pp. 761–766, 1998.
9. J. M. M. Schmitt and F. Favata, "Continuous heating of a giant x-ray flare on Algol," *Nature* **401**, pp. 44–46, 1999.

10. N. S. Brickhouse, "Dissecting the EUV spectrum of Capella," in *Astrophysics in the Extreme Ultraviolet*, S. Bowyer and R. F. Malina, eds., *IAU Coll.* **152**, pp. 105–112, 1996.
11. N. S. Brickhouse, "Spectral synthesis for high resolution spectra," in *Stellar Coronae in the Chandra and XMM-Newton Era*, F. Favata and J. J. Drake, eds., *ASP Conf.* **in press**, 2002.
12. S. Redfield, T. R. Ayres, J. L. Linsky, T. B. Ake, A. K. Dupree, R. D. Robinson, and P. R. Young, "Far Ultraviolet Spectroscopic Explorer survey of coronal forbidden lines in late-type stars," *Ap J* **in press**, 2002.
13. S. S. Vogt, A. P. Hatzes, A. A. Misch, and M. Kurster, "Doppler imagery of the spotted RS Canum Venaticorum star hr 1099 (V711 Tauri) from 1981 to 1992," *Ap J Supp.* **121**, pp. 547–589, 1997.
14. J.-F. Donati and A. C. Cameron, "Differential rotation and magnetic polarity patterns on AB Doradus," *MNRAS* **291**, pp. 1–19, 1997.
15. M. Jardine and Y. C. Unruh, "Coronal emission and dynamo saturation," *A&A* **346**, pp. 883–891, 1999.
16. N. S. Brickhouse and A. K. Dupree, "Extreme Ultraviolet Explorer observations of the W Ursa Majoris contact binary 44i Bootis: Coronal structure and variability," *Ap J* **502**, pp. 918–931, 1998.
17. J. J. Drake, J. M. Laming, and K. G. Widing, "Stellar coronal abundances. 2: The first ionization potential effect and its absence in the corona of Procyon," *Ap J* **443**, pp. 393–415, 1995.
18. J. J. Drake, N. S. Brickhouse, V. Kashyap, J. M. Laming, D. P. Huenemoerder, R. K. Smith, and B. J. Wargelin, "Enhanced noble gases in the coronae of active stars," *Ap J* **548**, pp. L81–L85, 2001.
19. A. C. Brinkman and et al., "First light measurements with the XMM-Newton reflection grating spectrometers: Evidence for an inverse first ionisation potential effect and anomalous Ne abundance in the coronae of HR 1099," *A&A* **365**, pp. L324–L328, 2001.
20. R. K. Smith, N. S. Brickhouse, D. A. Liedahl, and J. C. Raymond, "Collisional plasma models with APEC/APED: Emission-line diagnostics of hydrogen-like and helium-like ions," *Ap J* **556**, pp. L91–L95, 2001.
21. M. Audard, E. Behar, M. Gudel, A. J. J. Raassen, D. Porquet, R. Mewe, C. R. Foley, and G. E. Bromage, "The XMM-Newton view of stellar coronae: High-resolution x-ray spectroscopy of Capella," *A&A* **365**, pp. L329–L335, 2001.
22. A. C. Brinkman and et al., "First light measurements of Capella with the Low-Energy Transmission Grating Spectrometer aboard the Chandra X-ray Observatory," *Ap J* **530**, pp. L111–L114, 2000.
23. J.-U. Ness and et al., "Helium-like triplet density diagnostics. applications to Chandra LETGS x-ray observations of Capella and Procyon," *A&A* **367**, pp. 282–296, 2001.
24. R. Mewe, A. J. J. Raassen, J. J. Drake, J. S. Kaastra, R. L. van der Meer, and D. Porquet, "Chandra LETGS x-ray observations of Capella. temperature, density and abundance diagnostics," *A&A* **368**, pp. 888–900, 2001.
25. C. R. Canizares and et al., "High-resolution x-ray spectra of Capella: Initial results from the Chandra High-Energy Transmission Grating Spectrometer," *Ap J* **539**, pp. L41–L45, 2000.
26. T. R. Ayres, A. Brown, R. A. Osten, D. P. Huenemoerder, J. J. Drake, N. S. Brickhouse, and J. L. Linsky, "Chandra, EUVE, HST, and VLA multiwavelength campaign on HR 1099: Instrumental capabilities, data reduction, and initial results," *Ap J* **549**, pp. 554–577, 2001.
27. N. S. Brickhouse and J. J. Drake, "Coronal physics and the Chandra Emission Line Project," in *Astrophysical Plasmas: Codes, Models, and Observations*, J. Arthur, N. S. Brickhouse, and J. Franco, eds., *Rev. Mex. de Astron y Astrof* **9**, pp. 24–31, 2002.
28. G. A. Doschek, "Soft x-ray spectroscopy of solar flares: An overview," *Ap J Supp* **73**, pp. 117–130, 1990.
29. U. I. Safronova, A. A. Vasilyev, and R. K. Smith, "Satellite dielectronic spectra created from autoionizing 2lnlánd 1s2lnlẃith n=4-5," *Canadian J. Phys.* **78**, pp. 1055–1068, 2001.
30. C. J. Schrijver and M. J. Aschwanden, "Constraining the properties of nonradiative heating of the coronae of cool stars and the Sun," *Ap J* **566**, pp. 1147–1165, 2002.
31. N. S. Brickhouse, A. K. Dupree, and P. R. Young, "X-ray Doppler imaging of 44i Boo," *Ap J* **562**, pp. L75–L78, 2001.